Structural color in the Swallow Tanager (*Tersina viridis*): Using the Korringa-Kohn-Rostoker method to simulate disorder in natural photonic crystals

Christian D'Ambrosio
Universidad de Buenos Aires, Facultad de Ciencias Exactas y Naturales, Departamento de Física, Grupo de Electromagnetismo Aplicado, Buenos Aires, Argentina

Diana C. Skigin* and Marina E. Inchaussandague
Universidad de Buenos Aires, Facultad de Ciencias Exactas y Naturales, Departamento de Física, Grupo de Electromagnetismo Aplicado, Buenos Aires, Argentina and CONICET–Universidad de Buenos Aires, Instituto de Física de Buenos Aires (IFIBA), Buenos Aires, Argentina

Ana Barreira and Pablo Tubaro
División de Ornitología, Museo Argentino de Ciencias Naturales "Bernardino Rivadavia" MACN-CONICET, Av. Ángel Gallardo 470 (C1405DJR), Buenos Aires, Argentina

(Received 19 April 2018; published 4 September 2018)

The plumage of birds often exhibits attractive color effects produced by the interaction of light with the photonic microstructure present in the feather barbs and barbules. This microstructure constitutes a natural photonic crystal that rejects radiation of wavelengths contained within the band gap, which significantly alters the observed coloration depending on the incidence conditions. In spite of the high degree of regularity exhibited by the barb's microstructure of many species, the disorder present in these natural photonic crystals might modify the reflected response. In this paper, we address the problem of modeling the electromagnetic response of a quasiordered photonic structure, using an electromagnetic method only suitable for strictly periodic structures. In particular, we simulate the reflected response of the plumage of the Swallow Tanager (*Tersina viridis*) by two different approaches. On the one hand, we compute the reflected response by averaging reflectance spectra calculated by the Korringa-Kohn-Rostoker method for different geometrical parameters. We also apply the inner extinction approximation, which represents imperfections in the structure by adding a small imaginary part to the dielectric constant of the inclusions. The agreement between the experimental and the simulated results evidences the potential of the proposed methods to reproduce the electromagnetic response of natural photonic structures.

DOI: 10.1103/PhysRevE.98.032403

I. INTRODUCTION

Over millions of years of evolution, nature has developed an enormous variety of microstructures present in the cover tissues of animals and plants that interact with the incident light and give rise to attractive structural colors [1–5]. Optical mechanisms such as multilayer interference, scattering, and diffraction often govern the reflected response of such tissues, thus producing remarkable effects such as iridescence and metallic appearance. These features are also widely found in the plumage of birds [6–14]. The structural colors of avian feather barbs and barbules are generally produced by three-dimensional nanostructures composed of β-keratin and air. In many species of the *Thraupidae* family, such as *Tersina viridis* and *Dacnis cayana*, these nanostructures exhibit a sphere-type morphology that consists of a quasiordered arrangement of spheroidal air cavities in a β-keratin matrix [13,15]. Even though the distribution of air cavities within the host matrix is rather regular, it exhibits a certain degree of disorder, as expected for any natural structure, which gives rise to a complex reflected response. In addition, taking into account that macroscopic features such as the curvature of the barbs also contribute to the observed color, in some cases it is difficult to identify which is the dominant mechanism and how much the disorder present in the microstructure affects the electromagnetic response of an otherwise perfectly periodic structure.

Most of the works devoted to the study of structural color in birds' plumage applied two-dimensional (2D) Fourier analysis to estimate the reflected response of the microstructure [6–8]. Fourier analysis has proved to be a powerful tool to predict the spectral location of the main reflectance peak—located within the visible range—for many different species. Moreover, using the Fourier power spectra obtained from x-ray scattering experiments, in [16] the authors provide an explanation of the physical origin of the secondary peak based on double scattering within the short-range-order nanostructure. However, other methods have also been proposed to explain the observed color. For instance, a simple thin-film

*dcs@df.uba.ar

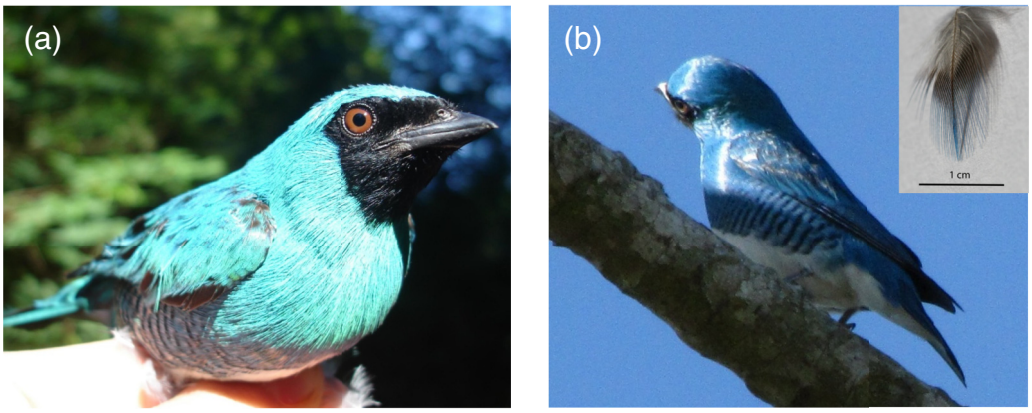

FIG. 1. Photographs of male individuals of *Tersina viridis* taken at different illumination-observation conditions. (a) The bird is illuminated from behind the camera; (b) the bird is illuminated from the left. The inset shows a single back feather of the *Tersina viridis* individual under study, which is deposited at the Museo Argentino de Ciencias Naturales "Bernardino Rivadavia," Argentina (collection code MACN-Or-32133).

interference model was sufficient to reproduce the essential characteristics of the color effect in pigeon feathers [11]. The plane-wave expansion method was employed to explain the structural color observed in peacock feathers [10], as well as in wild turkeys and violet-backed starlings [17], and in [9] the authors present a simple model that takes into account the submicron as well as the macroscopic features to explain the iridescence of the peacock plumage. More recently, the small-angle x-ray scattering (SAXS) method was proposed by Saranathan *et al.* to account for the 3D nature of the microstructure and its optical properties [13], and Igic *et al.* estimated the spectral peak position of *Lepidothrix iris* and *L. natterei* by approximating the underlying microstructure by a close-packed hexagonal array of air voids, and they used a multilayer model to compute the reflectance spectra [14].

In a recent paper, we have proposed the use of the Korringa-Kohn-Rostoker (KKR) method to simulate the electromagnetic response of the microstructure present in the feather barbs of *Tersina viridis* [15]. The KKR method is an efficient rigorous method for the calculation of the electromagnetic response of composite periodic structures formed by a stack of parallel layers of spheres periodically arranged in a 2D Bravais lattice [18–20]. Even though the spectral location of the main peak can be quite accurately reproduced by considering a perfectly regular arrangement, more subtle features of the reflectance spectrum, which appear due to the complexity and the irregularities of the actual biological microstructure, could not, in principle, be accounted for by the KKR method, only suitable to deal with regular lattices.

It is well known that essentially numerical electromagnetic methods capable of dealing with randomly distributed spheres in a host matrix, such as the finite elements or the finite-difference time-domain method, are computationally highly demanding. As a consequence, an appropriate simulation of the structural colors produced by biological structures constitutes a challenging task. One possibility to circumvent this disadvantage is to include disorder within the framework of a rigorous method originally developed for perfectly periodic structures. Dorado *et al.* introduced the effect of imperfections within the KKR method and modeled the response of a weakly disordered artificial opal by adding a small imaginary part to the dielectric constant of the spheres [inner extinction approximation (IEA)] [21–23]. These authors also proposed the average T-matrix approximation (ATA) as an alternative way of introducing disorder within the context of the KKR method, which takes into account the statistical distribution of sphere sizes and vacancy states in an artificial opal [24].

In this contribution, we propose two different techniques to simulate disorder in the sphere-type microstructures of avian feather barbs, namely an averaging technique and the IEA, and we show that the computed reflectance curves are in very good agreement with the experimental spectra.

The paper is organized as follows. In Sec. II we describe the sample under study, paying particular attention to the geometrical parameters of the microstructure responsible for the structural color. The results obtained applying the proposed techniques to simulate disorder are shown in Sec. III, where we also include a comparison with experimental spectra. Finally, concluding remarks are given in Sec. IV.

II. SAMPLE DESCRIPTION

The samples under study correspond to male individuals of *Tersina viridis*, which exhibit blue or green coloration depending on the illumination and observation conditions. As shown in Fig. 1, when the bird is illuminated from behind the camera, it looks turquoise (green-blue) [Fig. 1(a)], whereas if the observation direction is opposite to the illumination source, the bird appears blue [Fig. 1(b)]. It has been shown that the coloration of these feathers is of structural origin, and is produced by the interaction of light with the photonic microstructure present in the barbs located at the most external part of the feathers [see the inset of Fig. 1(b)] [15,25]. In Fig. 2(a), we show a transmission electron microscopy (TEM) image of a transversal cut of a barb of a male *Tersina viridis* individual. A detail of the spongy matrix is shown in Fig. 2(b), where a three-dimensional, quasiordered nanostructure composed of spherical air cavities immersed in a β-keratin matrix is observed. This structure, together with the curvature of the barb, is responsible for the color exhibited by the *Tersina viridis* plumage. In a previous work, we obtained the relevant

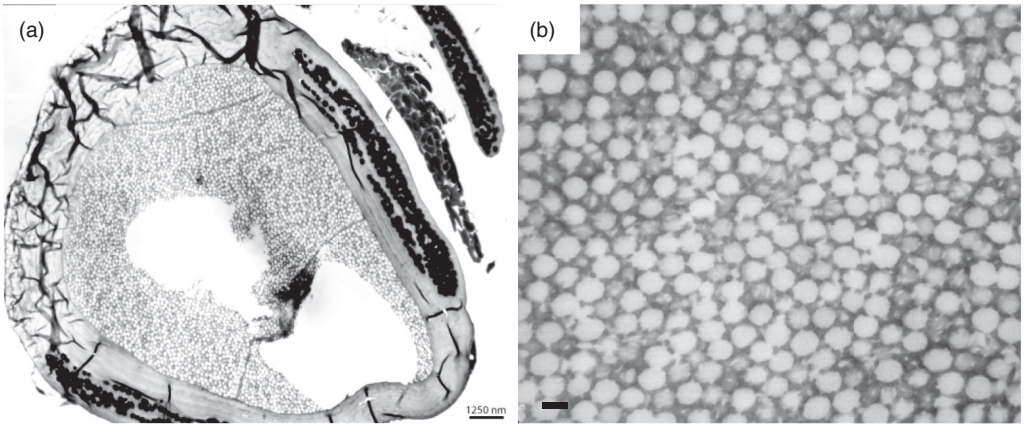

FIG. 2. (a) TEM image of a transversal cut of a barb of a male *Tersina viridis* individual (scale bar: 1.25 μm). (b) Detail of the spongy matrix composed of air spheres immersed in a β-keratin matrix (scale bar: 0.2 μm).

parameters of this microstructure from TEM images and a subsequent detailed statistical treatment. In Table I, we summarize the geometrical parameters of the structure and the refraction indices of its components [15].

According to the analysis of many TEM images, we considered that the type of arrangement that best reproduces this natural microstructure is a three-dimensional hexagonal lattice [15], as already reported for other species [14]. However, it is important to mention that the number of layers of spheres was highly dependent on the imaged section. In addition, it was very difficult to determine the number of layers in a given barb section due to the fragility of the samples, since part of the sample was always damaged or broken during preparation for TEM imaging.

III. RESULTS

In Fig. 3 we show the experimental reflectance spectrum taken with a coaxial fiber at approximately normal incidence with respect to the museum skin surface. Under this illumination-observation configuration, the bird's hue appears green-blue, as shown in Fig. 1(a). This spectrum was obtained as an average over 15 reflectance spectra that correspond to different parts of the back of the same investigated specimen. The method employed to perform the reflectance measurements is described in Ref. [25]. The measured spectrum reveals a bimodal reflectance profile of structurally colored feathers typical of certain species [14,26]. It exhibits a primary reflectance peak in the visible region ($\lambda \approx 560$ nm), and an additional peak in the ultraviolet (UV) ($\lambda \approx 380$ nm).

TABLE I. Relevant parameters of the microstructure responsible for the structural color in the plumage of male *Tersina viridis*.

Parameter	average value	error (sd)
radius of spheres (r)	86 nm	13 nm
distance between nearest neighbors (a)	240 nm	19 nm
refraction index of spheres (n_{air})	1	
refraction index of β-keratin (n_β) [13]	1.58	0.01

The numerical results shown below have been obtained using the KKR method [20], which permits the computation of the electromagnetic response of perfectly periodic arrangements of parallel layers of spheres. In the following figures, we present curves of reflectance as a function of the wavelength. The reflectance calculations were performed for both TE- and TM- (transverse-electric- and transverse-magnetic-) polarized light, which were then averaged to obtain the reflectance spectra for unpolarized light.

In Fig. 4 we plot the reflectance spectrum of the reference structure, i.e., a system formed by 34 layers of air spheres with $r = 86$ nm and $a = 240$ nm (average values measured from the TEM images, as listed in Table I) arranged in a hexagonal lattice and immersed in a β-keratin matrix ($n_\beta = 1.58$), illuminated by a normally incident plane wave. The curve exhibits a typical photonic crystal response, with a wide peak corresponding to a photonic band gap at wavelengths λ between 500 and 600 nm. In the context of structural coloration of birds' plumage, this kind of response is clearly a drawback of the model, as it exhibits characteristics that would only appear in the case of a perfectly periodic structure, which is not the case of natural structures. However, the spectral location of this band gap agrees very well with the position of the experimental primary peak. In addition, a reflectance

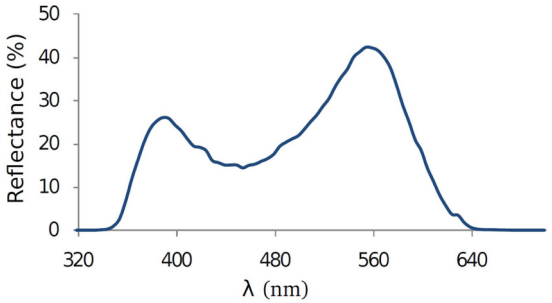

FIG. 3. Reflectance spectrum obtained by averaging 15 reflectance measurements performed on different parts of the back of the individual studied museum skin from which the investigated feather sample was obtained. Each spectrum was obtained at approximately normal incidence with respect to the skin surface.

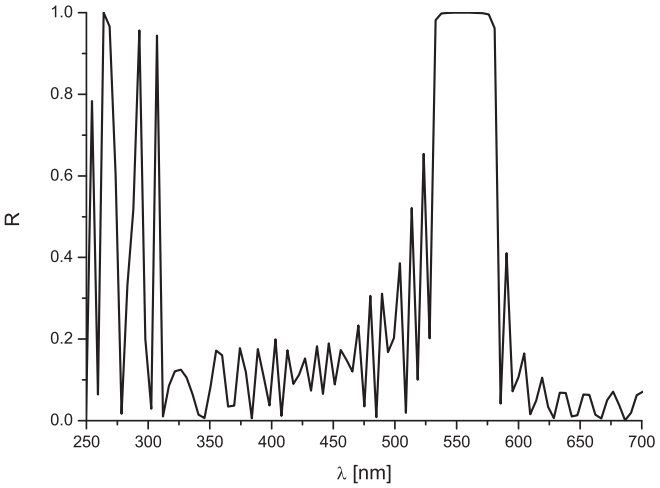

FIG. 4. Optical reflectance spectrum obtained by the KKR method for the reference structure: a multilayer hexagonal close-packed array (lattice constant $a = 240$ nm, separation between adjacent layers $z = \sqrt{2/3}a$, $r = 86$ nm) of air spheres in a β-keratin matrix ($n_\beta = 1.58$ and $\mu = 1$), considering 34 layers of spheres and normal incidence.

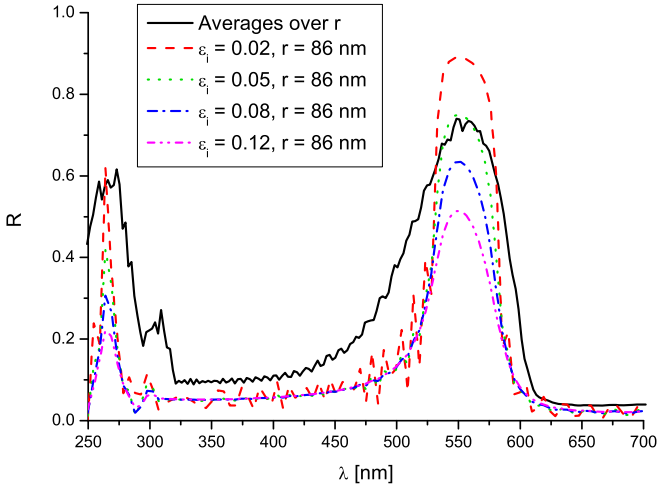

FIG. 5. Optical reflectance spectra obtained by the KKR method, employing two different approaches that take into account disorder within the structure: averaging 200 reflectance spectra corresponding to structures differing in the sphere's radius (black solid line), and using the IEA, i.e., adding a small imaginary part (ϵ_i) to the dielectric constant of air.

intensification can be identified within the UV region, around $\lambda = 275$ nm. As shown in Ref. [15], this enhancement could not be predicted by the single-scattering Fourier approach, which does not take into account higher-order contributions. By comparison of this calculated response and the experimental measurement (Fig. 3), it arises immediately that although the spectral location of the peak in the visible range is quite accurately predicted by the numerical results, there are other characteristics of the spectrum that are not accounted for by the ideal perfectly periodic model, such as the intensity and the shape of the peak. In addition, it is to be expected that the deviations of the natural structure from the ideally ordered system would provide a broadening of the reflectance peak and also a significant decrease of their intensity. Therefore, it becomes evident that any accurate model for the computation of the reflected response of the barb's tissue must somehow incorporate the disorder present in such photonic structures. In particular, note that to predict the observed color of the birds' plumage, it is necessary to take into account all the features of the reflectance spectrum, and not only the spectral location of the maxima.

We propose two different techniques to better estimate the reflectance response of the sample without using a highly computationally demanding tool. One of the approaches employed to compute the electromagnetic response of the disordered system is the inner extinction approximation, which has been previously applied to artificial opals with relative standard deviation in radius $\sigma_r^{\text{rel}} = \sigma_r / r_{\text{av}} \approx 0.05$ (r_{av} and σ_r are the average value and the standard deviation of the radius, respectively) [24]. The second approach, the averaging technique, consists in obtaining the reflectance curve of the actual quasiperiodic structure as an average over the reflectance curves of a set of perfectly regular structures in which one or more parameters are varied. According to the characteristics of the natural structure under study and to the uncertainties of the geometrical parameters measured from the TEM images, one selects the parameters and their variation ranges to be considered. In the case of *Tersina viridis*, one can make averages over the sphere radius, the distance between nearest neighbors, and/or the refraction indices of the materials involved. It is important to mention that averages have been previously proposed in the framework of structural color of birds' feathers. In Ref. [27], the authors obtain the reflectance spectrum of a barbule of an iridescent feather of a bird of paradise, as an average of the reflectance over 36 sections of this barbule, and this result is compared with the experimental spectrum, with highly satisfactory agreement.

As a first approach, in Fig. 5 we show the results obtained by the application of the IEA for different values of the imaginary part of the dielectric constant of the spheres, i.e., for $\epsilon_i = 0.02$, 0.05, 0.08, and 0.12, while the rest of the parameters are the same as those of Fig. 4. The IEA consists in computing the reflectance response of the disordered structure by calculating the reflectance of a single perfectly periodic structure, i.e., the reference structure, but including an artificial imaginary part to the dielectric constant of the spheres. The IEA is particularly suitable to model the electromagnetic response of spheres' structures with small variations in size and/or shape of the inclusions, and not in the lattice constant. As shown in Fig. 5, as ϵ_i increases the peak reflectance decreases, and the spectrum features smoothen as a result of diffuse scattering. However, the spectral location of the primary peak remains at the same wavelength, which is in very good agreement with the experimental curve (see Fig. 3). In addition, a secondary peak within the UV range is also revealed by the IEA curves.

In Fig. 5 we also show the reflectance spectrum obtained by averaging the reflectance responses of 200 regularly periodic structures with all the same parameters (given in Table I) except the sphere radius r (black solid line). In the simulations, the values of r were randomly generated according to a Gaussian distribution function with standard deviation σ_r. To apply the averaging technique, we have taken into account

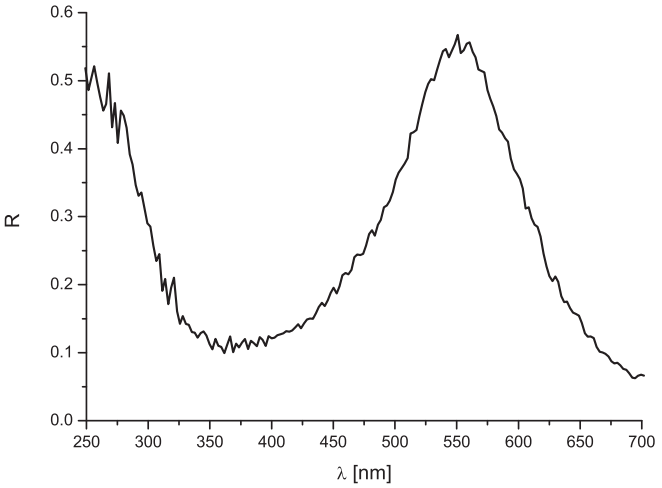

FIG. 6. Optical reflectance spectrum obtained by the KKR method, averaging 200 reflectance spectra corresponding to structures differing in the lattice constant.

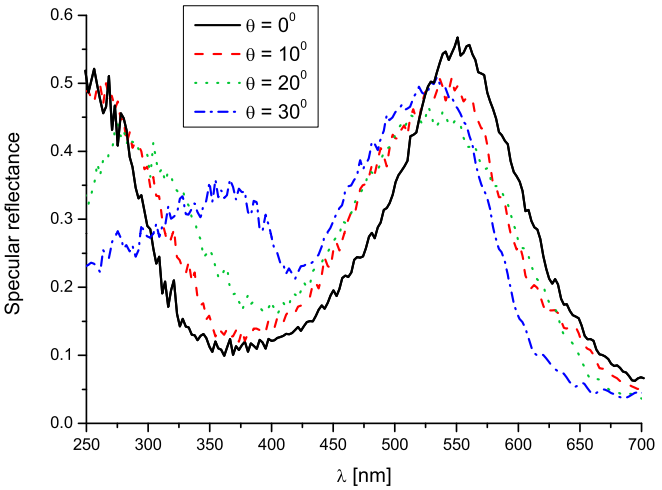

FIG. 7. Specular reflectance spectra for different incidence angles obtained by the KKR method, averaging 200 reflectance spectra corresponding to structures differing in the lattice constant.

that in the tissue of *Tersina viridis*, $\sigma_r^{\mathrm{rel}} \approx 0.15$ and $\sigma_a^{\mathrm{rel}} = \sigma_a/a_{\mathrm{av}} \approx 0.08$ (σ_a is the standard deviation in the values of the lattice constant a, and a_{av} is its average value), i.e., larger than for the artificial opals modeled in Ref. [24]. It is important to remark that σ_r not only reveals the actual variation of radius within the spongy matrix, but it also suffers from the errors associated with the measuring technique, which relies on transversal cut images of the barbs that eventually exhibit sphere slices that appear as spheres of smaller radius in the TEM images, or with an elongated cross section. On the other hand, the refraction indices of the spheres and the host matrix are well established [13], thus we have not varied these parameters in the simulations.

As can be observed by comparing this curve with the reference curve shown in Fig. 4, the effect of averaging is remarkable. On the one hand, the primary peak broadens and its intensity value decreases while keeping its spectral location at the expected wavelength according to the experimental curve. On the other hand, the highly oscillating behavior revealed by the spectrum of the reference structure in the UV range (Fig. 4) evolved in a clearly defined peak. By comparison between the results of the IEA and the averaging technique, the best matching between the average over 200 realizations and the IEA is obtained for $\epsilon_i = 0.05$. It is important to remark that the IEA is much less time-consuming than the averages technique, since it demands the computation of a single reflectance spectrum.

In Fig. 6 we show the reflectance spectrum obtained by averaging 200 spectra corresponding to perfectly periodic structures with the average parameters (see Table I), except the lattice constant a. The values of a for each of the structures were randomly generated according to a Gaussian distribution function that approximates the distribution of distances to nearest neighbors measured from the TEM images [15]. It can be observed that the primary reflectance peak broadens in relation to that of the reference structure spectrum (Fig. 4), and also in comparison with the peak obtained for the average curve over values of r (Fig. 5). In addition, the intensity of the reflectance peak decreased and it smoothed with respect to that of the perfectly periodic structure (Fig. 4). Also note that by averaging over the lattice constant a, the UV peak also arises as a well-defined peak. It is then clear that by applying either the averaging technique or the IEA, one can significantly improve the simulation of the measured reflectance spectrum. However, when comparing Fig. 6 with Fig. 3, we can notice that both curves do not match satisfactorily, especially in the spectral position of the secondary peak, which is at $\lambda \approx 380$ nm in the experimental curve and at $\lambda \approx 250$ nm in the simulated curve. If we take into account the experimental conditions of the measurement [25], which involves a finite-size light spot of a few millimeters, it becomes evident that the measured spectrum corresponds to a superposition of spectra for many different barbs, each with its own orientation and curvature, which imply different local incidence angles. As noticed by Yoshioka *et al.*, the macroscopic features of the barbs, such as the curvature in the transverse and longitudinal directions, modify the reflectance response of the feathers, especially the angular spectrum [9] and consequently the observed color. A blunt example of this is found in the boomerang-shaped barbules of the bird of paradise's breast feathers, which comprise three multilayer reflectors incorporated in a single structure to produce dramatic color changes during courtship display [28]. The curved microstructure can be regarded as a succession of smoothly tilted structures with respect to the incident light direction, and this results in the broadening of the reflectance peaks. When the curved barb is illuminated by a finite-size normally incident beam, the local angle of incidence varies along the barb, depending on its inclination, as indicated in the inset of Fig. 7. This angle increases from the center to the limits of the light spot, and with the curvature of the sample. Therefore, this scattering problem can be viewed as the superposition of many different problems corresponding to planar structures illuminated by oblique incidence. As a consequence, the scattering peak under multidirectional illumination is broader than

that under directional illumination, and the peak wavelength can be significantly shifted [29].

Then, to take into account the influence of the curvature within our model, we performed averaged simulations for different incidence angles. Note that as the incidence angle increases, diffraction orders other than the specular order start to appear for short-wavelength incidences. Then, to resemble the measurement conditions, for incidence angles different from 0° we plot the specular reflectance spectra. It is important to remark that for $\theta = 0^\circ$, the specular reflectance coincides with the total reflectance, since no higher diffraction orders are present for the whole range of wavelengths investigated. In Fig. 7 we plot the obtained specular reflectance spectra for incidence angles $\theta = 10^\circ$, 20°, and 30°. For comparison, we also include the curve for $\theta = 0^\circ$—already shown in Fig. 6. Notice that as θ increases, the main peak slightly shifts to shorter wavelengths; for $\theta = 30^\circ$ it is approximately at 500 nm. At the same time, the peak at shorter wavelengths redshifts. In particular, for $\theta = 30^\circ$ the reflectance peak appears between 350 and 400 nm.

According to the proposed model, light is specularly reflected from the structure, and this implies that as the angle of incidence increases, so does the observation angle, and consequently the angle between the incidence and the detection directions also increases. In this context, the curves of Fig. 7 show that the reflectance at shorter wavelengths increases with the angle formed between the incidence and the observation directions. Notice that within the visible range, i.e., for $\lambda > 380$ nm, the normal incidence curve has only a single peak at $\lambda \approx 550$ nm (green), and an enhancement at the blue region of the spectrum starts to appear for larger values of θ. Therefore, the relative weight of the blue components of the reflectance spectrum in relation to the green ones also increases at oblique incidence, which produces a color shift toward the blue, as observed in Fig. 1. These results are in line with the experimental curves shown in Fig. 2 of Ref. [26], which show that as the angle between the incidence and observation direction increases, the reflectance peak at the greens decreases and that at the blues increases. Taking into account all the above, we conclude that our numerical results provide the basis for a theoretical explanation of the color change in this species, based on the influence of oblique incidence components on the experimentally observed color.

IV. DISCUSSION AND CONCLUSIONS

We have proposed two different approaches to model the reflected response of natural photonic crystals such as those found in avian feather barbs: the averaging technique and the inner extinction approximation. Both techniques are based on the use of the KKR method, which is a rigorous electromagnetic method capable of simulating the response of composite periodic structures formed by a stack of parallel layers of spheres periodically arranged in a 2D Bravais lattice. We applied these methods to the simulation of the reflected response of a colored feather of a *Tersina viridis* male, which exhibits a bimodal reflectance spectrum. It was shown that both the averaging method and the inner extinction method are able to reproduce quite successfully the main characteristics of the reflectance spectra, i.e., the spectral location of the peaks, and their intensities and bandwidths. These characteristics could not be accounted for either by the single-scattering Fourier approach, widely used for the estimation of the reflected response of birds' plumage, or by the KKR simulation of the reference structure (perfectly periodic structure with average geometrical parameters).

It is also important to remark that the experimental measurement with which we compared the computed results is an average over 15 spectra, each of which was taken by directly approaching an optical fiber to the avian skin. Therefore, taking into account the solid angle that can enter the measuring fiber (many incidence angles), and also that the measurement was done over the whole skin, which includes many barbs with different orientations, the experimental result could not, strictly speaking, be compared with our simulations for normal incidence. To estimate the contribution of non-normal incidence angles, we performed simulations varying this angle and showed that the reflectance peaks shift in the respectively expected directions.

The main achievement of this work is to reveal the power of the KKR method as an efficient rigorous tool for the simulation of the reflected response of biological photonic tissues. However, in order to improve the representation of the response of such complex structures, further research should be done. One possibility is to consider the average over different parameters, including also the type of lattice as a variable. Another method that could also be implemented within the KKR method is the average T-matrix method, which has also proved to be successful to model disorder in artificial opals.

ACKNOWLEDGMENTS

D.S. and M.I. acknowledge partial support from Consejo Nacional de Investigaciones Científicas y Técnicas (CONICET PIP 112-201101-00451) and Universidad de Buenos Aires (UBACyT 20020150100028BA). A.B. and P.T. acknowledge partial support from Consejo Nacional de Investigaciones Científicas y Técnicas (CONICET PIP 112-201501-00637CO) and from Agencia Nacional de Promoción de Científica y Tecnológica PICT 2014-2154 and PICT 2015-3560.

[1] M. Srinivasarao, Nano-optics in the biological world: Beetles, butterflies, birds, and moths, Chem. Rev. **99**, 1935 (1999).

[2] A. Parker, 515 million years of structural color, J. Opt. A **2**, R15 (2000).

[3] P. Vukusic and J. R. Sambles, Photonic structures in biology, Nature (London) **424**, 852 (2003).

[4] S. Kinoshita, *Structural Colors in the Realm of Nature* (World Scientific, Singapore, 2008).

[5] S. Berthier, *Iridescences, The Physical Colours of Insects* (Springer Science+Business Media, LLC, France, 2007).

[6] R. Prum, R. Torres, S. Williamson, and J. Dyck, Coherent light scattering by blue feather barbs, Nature (London) **396**, 28 (1998).

[7] R. Prum, R. Torres, S. Williamson, and J. Dyck, Two-dimensional Fourier analysis of the spongy medullary keratin of structurally coloured feather barbs, Proc. R. Soc. London, Ser. B **266**, 13 (1999).

[8] R. O. Prum and R. Torres, Structural colouration of avian skin: Convergent evolution of coherently scattering dermal collagen arrays, J. Exp. Biol. **206**, 2409 (2003).

[9] S. Yoshioka and S. Kinoshita, Effect of macroscopic structure in iridescent color of the peacock feathers, Forma **17**, 169 (2002).

[10] Y. Li, Z. Lu, H. Yin, X. Yu, X. Liu, and J. Zi, Structural origin of the brown color of barbules in male peacock tail feathers, Phys. Rev. E **72**, 010902(R) (2005).

[11] H. Yin, L. Shi, J. Sha, Y. Li, Y. Qin, B. Dong, S. Meyer, X. Liu, L. Zhao, and J. Zi, Iridescence in the neck feathers of domestic pigeons, Phys. Rev. E **74**, 051916 (2006).

[12] R. O. Prum, E. R. Dufresne, T. Quinn, and K. Waters, Development of color-producing β-keratin nanostructures in avian feather barbs, J. R. Soc. Interf. **6**, S253 (2009).

[13] V. Saranathan, J. Forster, H. Noh, S. Liew, S. Mochrie, H. Cao, E. Dufresne, and R. Prum, Structure and optical function of amorphous photonic nanostructures from avian feather barbs: A comparative small angle X-ray scattering (SAXS) analysis of 230 bird species, J. R. Soc. Interf. **9**, 2563 (2012).

[14] B. Igic, L. D'Alba, and M. Shawkey, Manakins can produce iridescent and bright feather colours without melanosomes, J. Exp. Biol. **219**, 1851 (2016).

[15] C. D'Ambrosio, M. Inchaussandague, D. Skigin, A. Barreira, and P. Tubaro, Structural color in *Tersina viridis*, Opt. Pura Apl. **50**, 279 (2017).

[16] H. Noh, S. F. Liew, V. Saranathan, R. O. Prum, S. G. J. Mochrie, E. R. Dufresne, and H. Cao, Contribution of double scattering to structural coloration in quasiordered nanostructures of bird feathers, Phys. Rev. E **81**, 051923 (2010).

[17] C. M. Eliason, P. P. Bitton, and M. D. Shawkey, How hollow melanosomes affect iridescent color production in birds, Proc. R. Soc. London, Ser. B **280**, 1505 (2013).

[18] N. Stefanou, V. Yannopapas, and A. Modinos, Heterostructures of photonic crystals: Frequency bands and transmission coefficients, Comput. Phys. Commun. **113**, 49 (1998).

[19] V. Yannopapas, A. Modinos, and N. Stefanou, Optical properties of metallodielectric photonic crystals, Phys. Rev. B **60**, 5359 (1999).

[20] N. Stefanou, V. Yannopapas, and A. Modinos, Multem 2: A new version of the program for transmission and bandstructure calculations of photonic crystals, Comput. Phys. Commun. **132**, 189 (2000).

[21] L. A. Dorado, R. A. Depine, and H. Míguez, Effect of extinction on the high-energy optical response of photonic crystals, Phys. Rev. B **75**, 241101(R) (2007).

[22] L. A. Dorado, R. A. Depine, G. Lozano, and H. Míguez, Physical origin of the high energy optical response of three dimensional photonic crystals, Opt. Express **15**, 17754 (2007).

[23] L. A. Dorado, R. A. Depine, D. Schinca, G. Lozano, and H. Míguez, Experimental and theoretical analysis of the intensity of beams diffracted by three-dimensional photonic crystals, Phys. Rev. B **78**, 075102 (2008).

[24] G. Lozano, H. Míguez, L. Dorado, and R. Depine, Modeling the optical response of three-dimensional disorder structures using the Korringa-Kohn-Rostoker method, in *Optical Properties of Photonic Structures: Interplay of Order and Disorder*, edited by M. F. Limonov and R. M. De La Rue (CRC, Boca Raton, FL, 2012), Chap. 2.3.

[25] A. Barreira, Evolución de los patrones de coloración del plumaje en fruteros neotropicales, Ph.D. thesis, UBA (2011).

[26] A. Barreira, N. García, S. Lougheed, and P. Tubaro, Viewing geometry affects sexual dichromatism and conspicuousness of noniridescent plumage of Swallow Tanagers (Tersina viridis), The Auk **133**, 530 (2016).

[27] D. G. Stavenga, H. L. Leertouwer, D. C. Osorio, and B. Wilts, High refractive index of melanin in shiny occipital feathers of a bird of paradise, Light: Sci. Appl. **4**, e243 (2015).

[28] D. G. Stavenga, H. L. Leertouwer, N. Justin Marshall, and D. Osorio, Dramatic color changes in a bird of paradise caused by uniquely structured breast feather barbules, Proc. R. Soc. London, Ser. B **278**, 2098 (2011).

[29] H. Noh, S. F. Liew, V. Saranathan, S. G. J. Mochrie, R. O. Prum, E. R. Dufresne, and H. Cao, How noniridescent colors are generated by quasi-ordered structures of birds feathers, Adv. Mater. **22**, 2871 (2010).